



# VCU

Virginia Commonwealth University  
**VCU Scholars Compass**

---

Electrical and Computer Engineering Publications

Dept. of Electrical and Computer Engineering

---

2013

## Correlation between Si doping and stacking fault related luminescence in homoepitaxial m-plane GaN

S. Khromov  
*Linköping University*

B. Monemar  
*Linköping University*

Vitaliy Avrutin  
*Virginia Commonwealth University, vavrutin@vcu.edu*

*See next page for additional authors*

Follow this and additional works at: [http://scholarscompass.vcu.edu/egre\\_pubs](http://scholarscompass.vcu.edu/egre_pubs)



Part of the [Electrical and Computer Engineering Commons](#)

Khromov, S., Monemar, B., Avrutin, V., et al., Correlation between Si doping and stacking fault related luminescence in homoepitaxial m-plane GaN. *Applied Physics Letters*, 103, 192101 (2013). Copyright © 2013 AIP Publishing LLC.

---

Downloaded from

[http://scholarscompass.vcu.edu/egre\\_pubs/6](http://scholarscompass.vcu.edu/egre_pubs/6)

This Article is brought to you for free and open access by the Dept. of Electrical and Computer Engineering at VCU Scholars Compass. It has been accepted for inclusion in Electrical and Computer Engineering Publications by an authorized administrator of VCU Scholars Compass. For more information, please contact [libcompass@vcu.edu](mailto:libcompass@vcu.edu).

---

**Authors**

S. Khromov, B. Monemar, Vitaliy Avrutin, Hadis Morkoç, L. Hultman, and G. Pozina

# Correlation between Si doping and stacking fault related luminescence in homoepitaxial *m*-plane GaN

S. Khromov,<sup>1</sup> B. Monemar,<sup>1</sup> V. Avrutin,<sup>2</sup> H. Morkoç,<sup>2</sup> L. Hultman,<sup>1</sup> and G. Pozina<sup>1,a)</sup>

<sup>1</sup>Department of Physics, Chemistry, and Biology (IFM), Linköping University, S-581 83 Linköping, Sweden

<sup>2</sup>Department of Electrical Engineering and Physics Department, Virginia Commonwealth University, Richmond, Virginia 23284, USA

(Received 3 October 2013; accepted 20 October 2013; published online 4 November 2013)

Si-doped GaN layers grown by metal organic vapor phase epitaxy on *m*-plane GaN substrates were investigated by low-temperature cathodoluminescence (CL). We have observed stacking fault (SF) related emission in the range of 3.29–3.42 eV for samples with moderate doping, while for the layers with high concentration of dopants, no CL lines related to SFs have been noted. Perturbation of the SF potential profile by neighboring impurity atoms can explain localization of excitons at SFs, while this effect would vanish at high doping levels due to screening. © 2013 AIP Publishing LLC. [<http://dx.doi.org/10.1063/1.4828820>]

Homoepitaxial III-nitride based light emitting diodes (LEDs) and laser diodes show much better performance characteristics as well as a longer operational lifetime.<sup>1</sup> LEDs utilizing non-polar orientations of GaN are of high interest for further development of modern optoelectronics because in this geometry the device efficiency can be further improved due to reduction of the quantum-confined Stark effect.<sup>2,3</sup> However, the main obstacles in this case are those caused by lack of suitable native substrates; thus, the growth is usually performed on foreign substrate materials, which leads to a poor structural quality especially for highly doped layers. Today, Ge is considered as a promising dopant for *n*-type GaN. Ge occupies the Ga lattice sites causing only an insignificant stress in the lattice, which results in less cracking even for very high Ge concentrations in comparison with Si-doping.<sup>4</sup> It can be utilized for growth of non-polar and semi-polar GaN epilayers on silicon substrates, since such heteroepitaxial layers exhibit a high dislocation density and a high probability to form cracks. Even homoepitaxial growth of GaN on non-polar surfaces (*a*- or *m*-plane) requires additional process optimization to reduce a high density of structural defects such as basal plane stacking faults (SFs), known for limiting the output power of GaN LEDs grown along the *a*-axis.<sup>5</sup> Semi-polar orientations in III-nitride heterostructures have been shown to be more promising than polar orientations with respect to radiative properties of excitons because the dislocation density is lower in these directions.<sup>6</sup> From this point of view, homoepitaxial Si-doped GaN layers grown on semi-polar planes can be more favorable assuming lower density of structural defects, in particular, SFs. SFs of different geometries can sometimes be optically active and may lead to several features in the luminescence spectra in the region of 3.29–3.41 eV as was reported for the heteroepitaxial undoped GaN grown in *a*- and *m*-directions.<sup>7–10</sup> In mature undoped or *n*-type doped polar GaN layers, the SF density is low and can hardly be considered as a problem for electronic and optoelectronic devices. Correspondingly, in such samples, usually no SF-associated emission is present in the

luminescence spectra. On the other hand, SF-related lines have been detected in hetero- and homoepitaxially fabricated *c*-plane GaN doped with Mg.<sup>11,12</sup> However, no convincing cathodoluminescence (CL) lines related to the SF emissions have been found in most Mg-doped *m*-plane GaN, although electron microscopy analysis has confirmed a high density of both prismatic SFs (PSFs) and basal plane SFs (BSFs).<sup>13</sup> This points to a lack of clear understanding as to when and why SFs can be optically active in GaN. Since we have already reported results concerning luminescence of SFs in polar and non-polar homoepitaxial GaN doped by Mg, it is deemed natural to extend investigations to nonpolar homoepitaxial GaN layers with other types of dopants. Thus, in this Letter, we report on the correlation between impurity levels and optical activation of SFs in Si-doped GaN layers grown on *m*-plane GaN substrates.

GaN layers of thickness  $\sim 1 \mu\text{m}$  were grown by metal organic vapor phase epitaxy (MOVPE). Samples were doped by Si with varying concentrations in the range of  $2 \times 10^{17}$  and  $5 \times 10^{18} \text{ cm}^{-3}$  as determined by secondary ion mass spectrometry (SIMS). The growth was done on *m*-plane GaN substrates starting with an undoped  $1 \mu\text{m}$  GaN buffer layer. Freestanding GaN substrates with threading dislocation density of  $\sim 5 \times 10^6 \text{ cm}^{-2}$  were provided by Kyma Technologies. Substrates were grown by halide vapor phase epitaxy (HVPE) in the *c*-direction and then cut and polished along the *m*-plane. Cross-sectional TEM analysis was done with a high resolution FEI Tecnai G2 200 keV FEG instrument. CL spectra were measured using a MonoCL4 system integrated with a LEO 1550 Gemini scanning electron microscope (SEM) and equipped with a liquid-He-cooled stage for low-temperature experiments performed at 5 K. The typical acceleration voltage for this study was 10 kV. A fast CCD detection system and a Peltier cooled photomultiplier tube were used for spectral acquisition and imaging.

A cross-sectional TEM micrograph shown in Fig. 1(a) reveals that the studied *m*-plane GaN samples suffer from a rather high density of BSFs ( $\sim 2 \times 10^4 \text{ cm}^{-1}$ ) propagating the entire layer towards the surface even for samples with relatively low doping levels. Besides BSFs, PSFs have also been observed as illustrated in Fig. 1(b). Most of the defects were

<sup>a)</sup>galia@ifm.liu.se

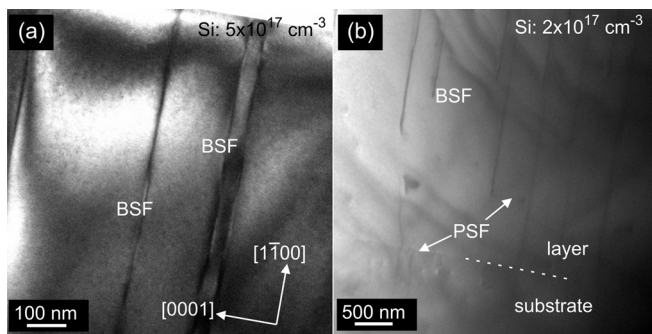


FIG. 1. Cross-sectional TEM images of *m*-plane GaN samples doped by Si with concentration (a)  $5 \times 10^{17} \text{ cm}^{-3}$  and (b)  $2 \times 10^{17} \text{ cm}^{-3}$ . The interface region between substrate and buffer is shown in (b). Arrows show the crystallographic directions.

likely formed during the nucleation and coalescence stages at the interface region between the buffer and the nonpolar GaN substrate.

Samples with morphology influenced by structural defects can be investigated by CL *in-situ* SEM. CL measurements taken over a typical area  $\sim 100 \times 100 \mu\text{m}$  reveal a clear dependence of the near band gap emission on Si concentration in GaN layers as depicted in Fig. 2. Although the evolution of the luminescence at doping concentrations around the Mott transition (at carrier concentrations of  $\sim 2\text{--}3 \times 10^{18} \text{ cm}^{-3}$ , Ref. 14) is a subject of separate work, it is worthwhile to point out here that below the Mott limit we observe excitonic rather than electron-hole plasma related transitions. For our samples, it means that the CL peak at  $\sim 3.47 \text{ eV}$  is due to the donor bound exciton (DBE) emission except for the layer with Si concentration of  $\sim 5 \times 10^{18} \text{ cm}^{-3}$ , where a high energy tail shows a small deviation in its shape explained by a competition of two effects: (i) the band-gap renormalization causing a red shift and (ii) the reduction of the exciton binding energy due to screening resulting in a blue shift. In the latter case, the position of the A exciton is at  $\sim 3.48 \text{ eV}$ , i.e., very close to the DBE peak in the lower doped samples. As seen in Fig. 2, we have not observed any additional lines related to the defect luminescence (i.e., SFs) in the region 3.29–3.42 eV for GaN samples doped with Si above  $\sim 10^{18} \text{ cm}^{-3}$  despite that SFs

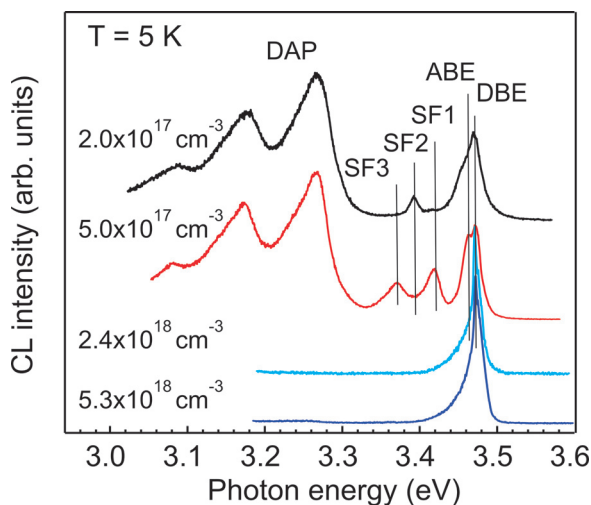


FIG. 2. Low-temperature CL spectra measured for samples with different Si concentration.

influence the sample morphology. Such luminescence spectra dominated mainly by the DBE line are typical for most *n*-type GaN of relatively high quality (undoped or Mg-doped with concentrations below  $2 \times 10^{18} \text{ cm}^{-3}$ ) grown in the *c*-direction.<sup>12,15</sup> In contrast, CL spectra are different for the GaN layers having lower Si concentrations in the range of  $2\text{--}5 \times 10^{17} \text{ cm}^{-3}$ . Unexpectedly, besides the DBE line, a well-resolved emission of the acceptor bound exciton (ABE) at  $\sim 3.46 \text{ eV}$  and a strong donor-acceptor pair (DAP) recombination line at  $\sim 3.26 \text{ eV}$  with two phonon replicas have been detected. Additionally, three rather narrow emission lines with relative intensities depending on samples and positions have been found in the region of defect luminescence: at  $\sim 3.42 \text{ eV}$  (SF1), at  $\sim 3.39 \text{ eV}$  (SF2), and at  $\sim 3.37 \text{ eV}$  (SF3). The emission within the range of 3.39–3.42 eV was previously identified as being related to BSF,<sup>7–10,16</sup> while the 3.37 eV peak is close to the feature at 3.34 eV related to PSFs in heteroepitaxial *a*-plane GaN.<sup>7</sup> The origin of these lines is in accordance with these identifications as it is confirmed by spatially resolved CL data presented in Fig. 3. However, as already mentioned above, we have not found the SF-related luminescence in the samples with Si doping exceeding  $10^{18} \text{ cm}^{-3}$ . In spite of this, we can observe SFs in SEM images and also in CL images, albeit as non-radiative regions in this case and in the layers. To illustrate our observations, an SEM image together with panchromatic CL (PCL) mapping for the layer doped with Si concentration of  $2.4 \times 10^{18} \text{ cm}^{-3}$  is shown in Figs. 3(a) and 3(b), respectively. Despite that, the PCL is very inhomogeneous reflecting the presence of structural defects, a corresponding CL spectrum revealed no SF-related lines as seen in Fig. 2. The same observation was noted for all the other GaN layers with high doping level. In contrast, for samples with

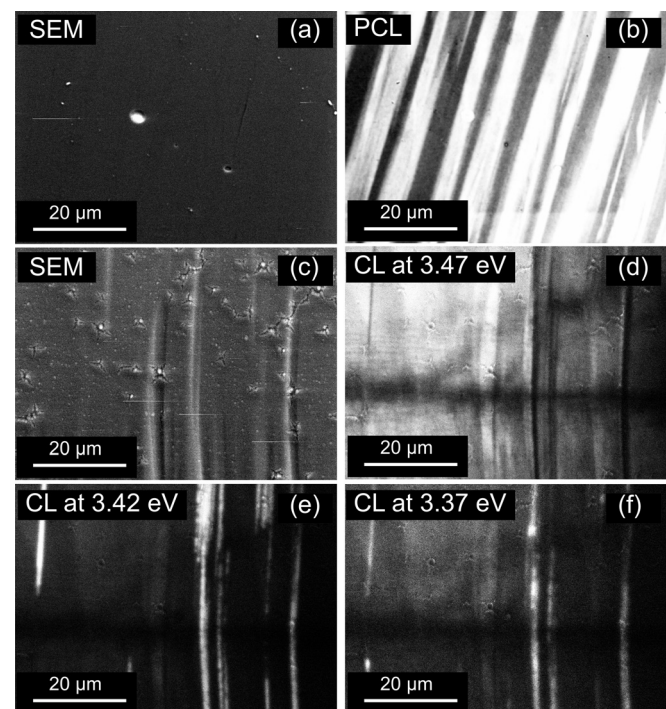


FIG. 3. SEM (a) and PCL (b) images of the GaN layer doped with Si at  $\sim 2.4 \times 10^{18} \text{ cm}^{-3}$ , (c) SEM images for the sample with Si concentration of  $5 \times 10^{17} \text{ cm}^{-3}$  with corresponding monochromatic CL images taken at different photon energies of 3.47 eV (d), 3.42 eV (e), and 3.37 eV (f).



lower Si concentrations, SFs are found to be optically active. Figs. 3(c) and 3(d) show a SEM image together with CL map measured at the DBE energy of 3.47 eV for the GaN layer with Si level of  $5 \times 10^{17} \text{ cm}^{-3}$ . It is clear from the figure that at this energy the SFs are revealed as dark features. However, two examples of CL mapping taken at photon energies related to SF1 (3.42 eV) and SF3 (3.37 eV) show a bright contrast (i.e., higher CL intensities) in the areas where the SFs are localized, as seen in Figs 3(e) and 3(f), respectively. The elongated shape of the CL contrast at 3.42 eV confirms that this emission is related to a BSF. The identification of the 3.37 eV line as related to PSFs can also be validated, since the bright contrast in CL is non-uniform along the BSFs (for example, it is stronger at some edges of the BSFs) reflecting the PSFs geometry to be likely of the connecting intrinsic  $I_T$ -BSFs in nature.<sup>17</sup>

Before we discuss the reason behind the optical activation of the SFs, we would like to present details of the selective CL analysis for the GaN layer with Si concentration of  $2 \times 10^{17} \text{ cm}^{-3}$  shown in Fig. 4. At the chosen area with clearly observed SFs (SEM image, Fig. 4(a)), the electron beam was focused at three different points numbered 1, 2, and 3. Although the focusing area is only over several nm, the excitation volume is about  $\sim 1 \mu\text{m}$  in diameter, thus, the signal is not perfectly selective. However, the data unequivocally show an enhanced contribution of the SFs related emissions in CL spectra when the detection is localized to SFs (point 1 and 2). An additional feature at  $\sim 3.3 \text{ eV}$  (PD)

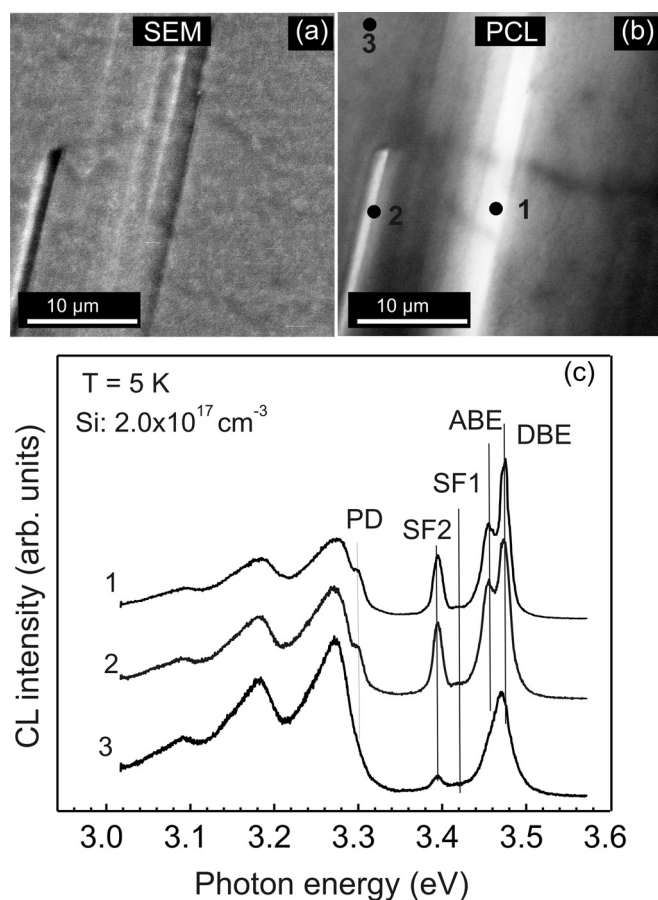


FIG. 4. SEM image (a) together with PCL map (b) for the GaN layer with Si concentration of  $2.4 \times 10^{17} \text{ cm}^{-3}$ . (c) CL spectra at 5 K detected at localized spots indicated in (b) with points 1, 2, and 3, respectively.

known as being related to partial dislocation terminating BSFs<sup>7</sup> was recently assigned to extrinsic BSFs.<sup>18</sup> The intensity of the SF related lines (SF2 and PD) is significantly smaller for point 3, where no visible defects have been observed in SEM.

The main conclusion of our present investigation is as follows: a SF-related luminescence has been observed in CL spectra only for such concentrations of donors and acceptors in GaN, when the typical ABE lines together with the DAP recombination were also observed. This suggests that for the studied Si-doped *m*-plane GaN samples the background residual acceptor concentration is likely higher than in *c*-plane GaN, which is reasonable since the incorporation of Mg in *m*-plane (10-10) is more favorable.<sup>19</sup> The unintentional Mg-doping of  $\sim 10^{16} \text{ cm}^{-3}$  (according to SIMS, which is, however, close to the detection limit) is presumably related to the well-known Mg memory effect in MOVPE growth of GaN.<sup>20</sup>

Now the data can be consistently explained:

- (i) SFs, especially BSFs, can be described as three monolayers of cubic GaN, surrounded by wurtzite GaN, thus, forming a QW without any well-width fluctuations and, consequently, without any in-plane localization for electrons.<sup>21</sup> There is also no confinement for holes due to a small valence band offset of  $\sim 0.07 \text{ eV}$ .<sup>22</sup> In the presence of a nearby impurity (donor and/or acceptor), there is a perturbation of the band potential in such a way that carrier confinement can be realized. That means that free excitons can now be trapped by such SFs in the vicinity of impurities and the exciton binding energy will depend on the distance from the impurity to the BSF plane.<sup>21</sup>
- (ii) For *n*-type samples with moderate donor concentrations, free excitons are bound to the most abundant impurities (Si and also O donor), and thus, the luminescence spectra are dominated by typical DBE lines and also by excitons bound to the impurity-BSF complex (here, likely to the donor-BSF system). The binding energy can vary due to different distances to BSF and/or different impurities, which may account for the observation of several luminescence lines related to BSF.
- (iii) In highly doped GaN with carrier concentrations above the Mott limit, the Coulomb interaction is screened thus annihilating the exciton localization to the donor-BSF complexes. In this case, BSFs will no more be optically active.

In summary, *m*-plane Si-doped GaN layers grown by MOCVD on GaN substrates were studied by low-temperature CL *in-situ* SEM to understand any correlation between doping level and/or dopant specie and the SF-related emission. We have found that SFs are optically active in GaN samples with moderate doping concentrations while for highly doped GaN layers no luminescence related to extended structural defects was observed. The effect is explained by a perturbation of the BSF potential profile in the vicinity of impurity atoms in such a way that exciton localization can be realized. On the other hand, screening of the charge carrier interaction at high doping results in

vanishing of the localization and thus no SF-related CL is present.

This work was supported by the Swedish Energy Agency and the Swedish Research Council (VR). The Knut and Alice Wallenberg Foundation supported the Electron Microscopy Laboratory at Linköping operated by the Thin Film Physics Division.

<sup>1</sup>I. Akasaki, *J. Cryst. Growth* **300**, 2 (2007).

<sup>2</sup>*Nitrides with Non-polar Surfaces: Growth, Properties and Devices*, edited by T. Paskova (Wiley-VCH, Weinheim, 2008).

<sup>3</sup>J. S. Speck and S. F. Chichibu, *MRS Bull.* **34**, 304 (2009).

<sup>4</sup>P. R. Hageman, W. J. Schaff, J. Janinski, and Z. Liliental-Weber, *J. Cryst. Growth* **267**, 123 (2004).

<sup>5</sup>K. H. Baik, Y. G. Seo, S.-K. Hong, S. Lee, J. Kim, J.-S. Son, and S.-M. Hwang, *IEEE Photon. Technol. Lett.* **22**, 595 (2010).

<sup>6</sup>D. Rosales, T. Bretagnon, B. Gil, A. Kahouli, J. Brault, B. Damilano, J. Massies, M. V. Durnev, and A. V. Kavokin, *Phys. Rev. B* **88**, 125437 (2013).

<sup>7</sup>R. Liu, A. Bell, F. A. Ponce, C. Q. Chen, J. W. Yang, and M. A. Khan, *Appl. Phys. Lett.* **86**, 021908 (2005).

<sup>8</sup>J. Mei, S. Srinivasan, R. Liu, F. A. Ponce, Y. Narukawa, and T. Mukai, *Appl. Phys. Lett.* **88**, 141912 (2006).

<sup>9</sup>T. B. Wei, J. K. Yang, Q. Hu, R. F. Duan, Z. Q. Huo, J. X. Wang, Y. P. Zeng, G. H. Wang, and J. M. Li, *J. Cryst. Growth* **314**, 141 (2011).

<sup>10</sup>I. Tischer, M. Feneberg, M. Schirra, H. Yacoub, R. Sauer, K. Thonke, T. Wunderer, F. Scholz, L. Dieterle, E. Müller, and D. Gerthsen, *Phys. Rev. B* **83**, 035314 (2011).

<sup>11</sup>G. Pozina, P. P. Paskov, J. P. Bergman, C. Hemmingsson, L. Hultman, B. Monemar, H. Amano, and A. Usui, *Appl. Phys. Lett.* **91**, 221901 (2007).

<sup>12</sup>S. Khromov, C. Hemmingsson, H. Amano, B. Monemar, L. Hultman, and G. Pozina, *Phys. Rev. B* **84**, 075324 (2011).

<sup>13</sup>S. Khromov, B. Monemar, V. Avrutin, X. Li, H. Morkoc, L. Hultman, and G. Pozina, *Appl. Phys. Lett.* **100**, 172108 (2012).

<sup>14</sup>F. Binet, J. Y. Duboz, J. Off, and F. Scholz, *Phys. Rev. B* **60**, 4715 (1999).

<sup>15</sup>B. Monemar, P. P. Paskov, T. Paskova, J. P. Bergman, G. Pozina, W. M. Chen, P. N. Hai, I. A. Buyanova, H. Amano, and I. Akasaki, *Mater. Sci. Eng., B* **93**, 112 (2002).

<sup>16</sup>P. Corfdir, P. Lefebvre, J. Levrat, A. Dussaigne, J.-D. Ganière, D. Martin, J. Ristić, T. Zhu, N. Grandjean, and B. Deveaud-Plédran, *J. Appl. Phys.* **105**, 043102 (2009).

<sup>17</sup>Y. Arroyo Rojas Dasilva, T. Zhu, D. Martin, N. Grandjean, U. Jahn, and P. Stadelmann, *J. Cryst. Growth* **327**, 6 (2011).

<sup>18</sup>J. Lähnemann, O. Brandt, U. Jahn, C. Pfüller, C. Roder, P. Dogan, F. Grosse, A. Belabbes, F. Bechstedt, A. Trampert, and L. Geelhaar, *Phys. Rev. B* **86**, 081302(R) (2012).

<sup>19</sup>J. E. Northrup, *Phys. Rev. B* **77**, 045313 (2008).

<sup>20</sup>H. Xing, D. S. Green, H. Yu, T. Mates, P. Kozodoy, S. Keller, S. P. Denbaars, and U. K. Mishra, *Jpn. J. Appl. Phys., Part 1* **42**, 50 (2003).

<sup>21</sup>P. Corfdir, P. Lefebvre, J. Ristić, J.-D. Ganière, and B. Deveaud-Plédran, *Phys. Rev. B* **80**, 153309 (2009).

<sup>22</sup>C. Stampfl and C. G. Van de Walle, *Phys. Rev. B* **57**, R15052 (1998).